

PAPER • OPEN ACCESS

Static Analysis of the Last Stage Low Pressure Steam Turbine Blade to Improve Blade twist Angle

To cite this article: Abolaji Joseph Omosanya *et al* 2021 *IOP Conf. Ser.: Mater. Sci. Eng.* **1107** 012056

View the [article online](#) for updates and enhancements.

You may also like

- [Leading edge topography of blades—a critical review](#)
Robert J K Wood and Ping Lu
- [Water droplet erosion of stainless steel steam turbine blades](#)
H S Kirols, D Kevorkov, A Uihlein et al.
- [Research on surface damage detection of wind turbinebladebased on machine vision](#)
Yu Wang and Li Zou



ECS Membership = Connection

ECS membership connects you to the electrochemical community:

- Facilitate your research and discovery through ECS meetings which convene scientists from around the world;
- Access professional support through your lifetime career;
- Open up mentorship opportunities across the stages of your career;
- Build relationships that nurture partnership, teamwork—and success!

Join ECS!

Visit electrochem.org/join



Static Analysis of the Last Stage Low Pressure Steam Turbine Blade to Improve Blade twist Angle

Abolaji Joseph Omosanya^{1,2*}, Esther Titilayo Akinlabi³ and Joshua Olusegun Okeniyi^{1,4}

¹Department of Mechanical Engineering Science, University of Johannesburg, Johannesburg, South Africa.

²Factory Projects, Nestle Nigeria Plc, Agbara Factory, Ogun State, Nigeria.

³Pan Africa University for Life and Earth Sciences Institute, Ibadan, Nigeria.

⁴Department of Mechanical Engineering, Covenant University, Ota, Ogun State, Nigeria.

Corresponding Author; deenkelson@gmail.com

Abstract-

Demand for electricity is growing continuously and the production is still based on limited sources of energy, mainly the turbomachinery, which include basically the steam and gas turbines. Turbomachinery is responsible for about 80% of the electricity generated worldwide. A large variety of turbine blade geometries are in use today, however, there is no specific attempt made to compare them based on performance.

This paper presents a study on the effect of the twist angle of the steam turbine blade on different choice blade materials. For the study, the aerodynamic and static loading of the 19th stage low pressure turbine blade of Egbin thermal power station was evaluated. Static analysis based on computational fluid dynamics (CFD) was used to simulate the conditions of the turbine blade during normal operating conditions. Alternative materials (such as stainless steel 316, Titanium alloy) and varying twist angles were observed to be showing different forms of results in the simulation on ANSYS. From these, an optimized twist angle was generated using Response Surface Optimization on ANSYS RSO, and the consequent results were discussed.

Key words: Turbine blade, Blade twist angle, CFD, ANSYS.

1. Introduction

In the last forty years, new insight has been drawn, from several research works, towards improving industrial steam turbines using computer simulations and laboratory experimentation of turbine systems [1]. These research works and studies have brought about the development of new and more durable materials like the Titanium alloy for turbine blades. Also, new manufacturing processes to develop more efficient and reliable steam turbines have been designed. For instance, the reported work in [2] explained that design of the steam turbine in recent years has allowed for inlet temperatures of the steam turbine to be increased up to 620 °C. Important parts of the turbomachinery that require attention in their design are the moving parts, which is consisted of the rotor blades and the shafts upon which the blades are mounted [3] [4]. These parts are exposed to both steady and dynamic stresses from the steam impacting upon them. The structural integrity and reliability of these parts have a direct effect on the reliability of the turbine engine. The turbine blade is the most important element of the steam power generation system. It is responsible for the conversion of the pressure energy of the steam to rotational kinetic energy of the rotor. Based on how the steam interacts with the blades, turbine blades can be classified as impulse or reaction [5]. It is necessary to



note that the shape, size and material of turbine blades vary all through the various stages of the steam turbine. The long length of the low-pressure last stage turbine blade exposes it to higher level of stress and structural issues such as Von Mises stress, large centrifugal stress, low rigidity and high Mach number flow [6]. Nagaraju et al, in [7], explained the various types of failures experienced by the turbine blade in a steam power generation plant. The failure mechanisms include excessive stress, centrifugal stress, steam induced stress - steady state and alternating, impact stress, low cycle fatigue, thermal fatigue, creep stress and resonant vibration. Twisted blades increase the velocity and while this makes the blades more efficient [8], it exposes the blade to the stress inducing failure mechanisms that had been identified in studies. Despite this, however, there is dearth of studies on the static analysis of the last stage low pressure steam turbine blade, especially, for improving the blade twist angle towards attaining increased velocity. No research work has been carried out concerning this on the Egbin thermal power station, in Nigeria. For this reason, this paper employs the last stage low pressure turbine blade of the Egbin thermal power station as a case study for the research on the static analysis of the last stage low pressure steam turbine blade, for improving the blade twist angle for that system. Presently, the blade being studied has a twist angle of 34 degrees and was made of 12 Chromium Stainless steel materials.

2. Model and Methodology

2.1 The CFD Simulation Software

The multipurpose computational fluid dynamics commercial simulation software, ANSYS is used in this work for the numerical analysis and study. The section of the software used for this work is the ANSYS Static Structural. The ANSYS Static Structural is used for the structural analysis of the blade under the given operating conditions. ANSYS, generally, operates by following the workflow of pre-processing - geometry creation and discretization (meshing), design physics set-up and solution, and post-processing. Due to the goal of optimum design of the steam turbine blade, a design exploration process – Design Xplorer – was employed. This solves generated output parameters, which are generated by the design of experiments option. Furthermore, response surfaces of outputs are developed, and then, these generated response surfaces of output parameters are used to find points that optimize the performance of the turbine blade geometry. Figure 1 below presents a typical ANSYS Workbench project schematic that includes the optimization process that is being employed for the turbine blade analysis in the present study.

2.2 The 3D Model and Mesh

The geometry was created in the ANSYS Workbench, which is a CAD tool function in ANSYS. Figure 2 shows the 3D model of the turbine blade. The coordinates were generated, which forms a curve that represents the shape of the blade. These points or coordinates were imported into the ANSYS Workbench in the .txt document type for the generation of the 2D profile. The 3D geometry was formed using the SKIN (or LOFT) command. With the geometry being a twisted profile along its longitudinal axis, the top section of the blade is inclined to the horizontal x-axis by 34°, which gives it the twisted shape.

The 3D discretization for the study and analysis of the static structural properties of the steam turbine blade was also performed using an unstructured mesh as seen in Figure 3. The element size used was 0.005 while the number of elements in the computational domain is 44918 with 83026 nodes.

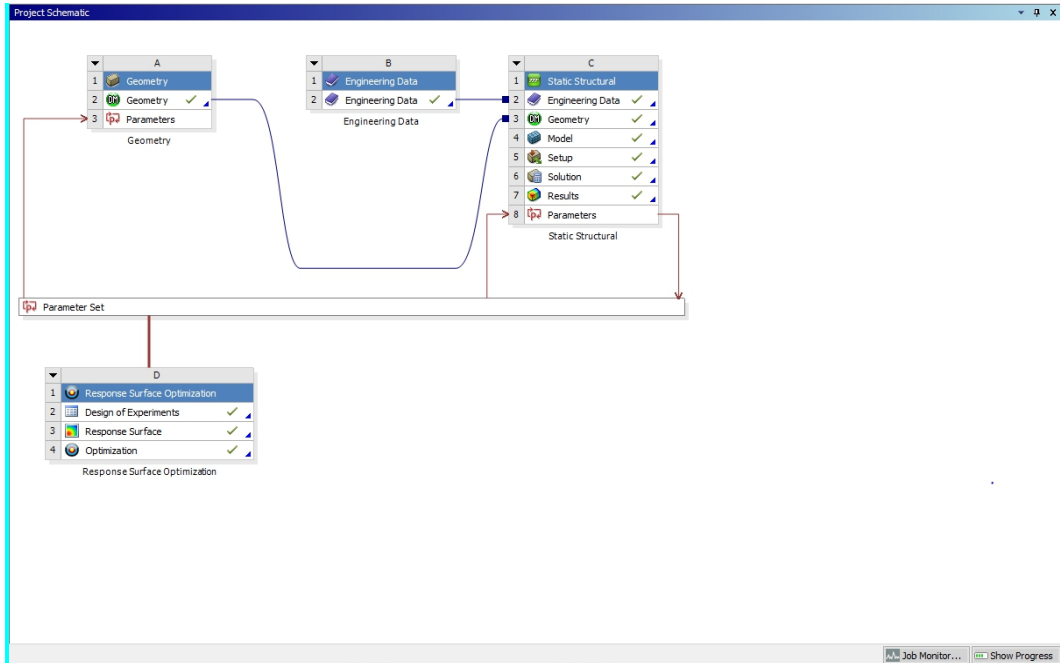


Figure 1: A Typical Analyse Workbench Schematic

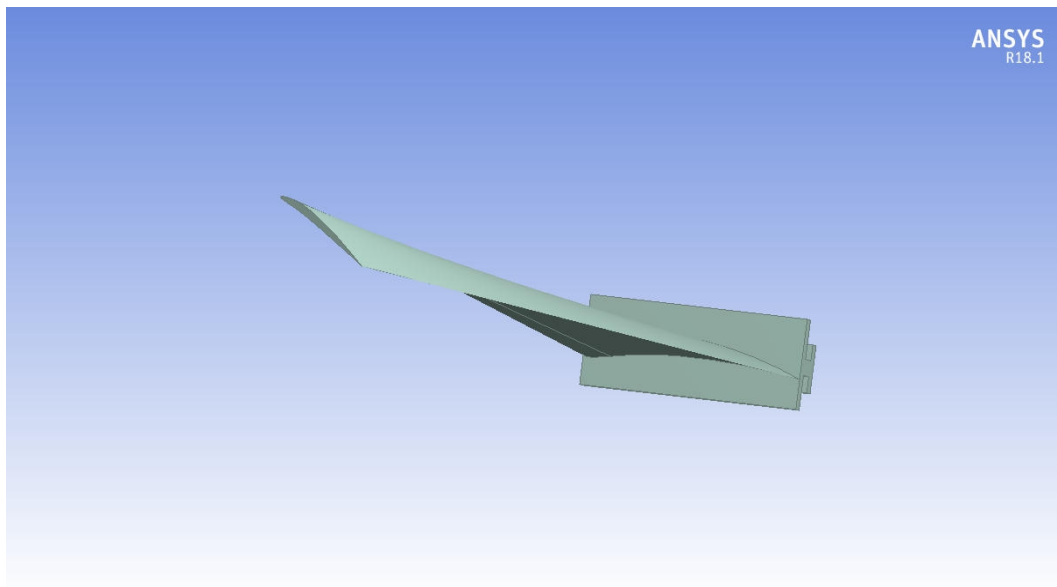


Figure 2: The 3D Model with Blade Hub

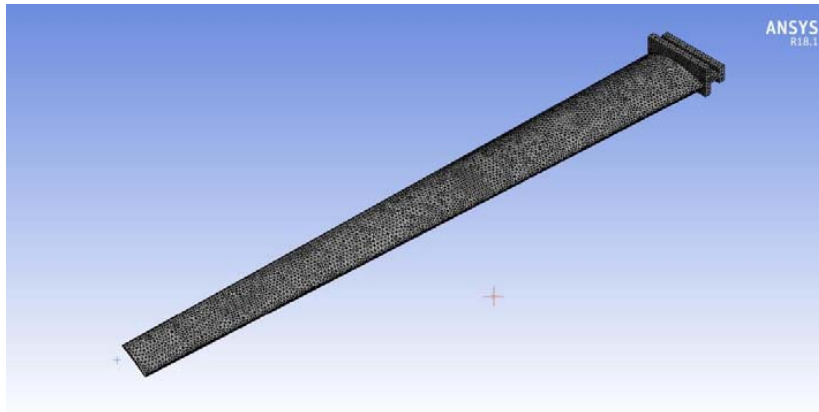


Figure 3: The unstructured 3D mesh

2.3 Response Surface Methodology

The response surface methodology (RSM) consists of mathematical and statistical approaches used in the development of an adequate functional relationship between a response of interest, $f(x)$ and several design (input) variables denoted by x_n . By careful design of experiments, the objective was to optimize a response (output variable), which is influenced by several input design parameters. In [9], Anderson-Cook et al gave a detailed explanation of the methodology. They highlighted that the RSM has three main objectives, which includes optimisation of the response output, mapping a response surface over a region of interest and selection of operating conditions to achieve customer requirements or specification. Also, in [10], Venter et al gave the advantages of using the response surface methodology for applications of design optimization. Response surface methodology, as a design optimization tool, aims at effective reduction in: the cost of computational fluid dynamics analyses, the numerical noise involved and the time needed for executing the numerical analyses.

2.4 Boundary Condition

From the turbine operational data from Egbin thermal station, the steam working velocity was calculated to be 34 m/s. Also, the pressure of the steam entering the low-pressure turbine, where the 19th stage blade is situated, is approximately 198 kPa. The materials employed for the static structural analysis of the blade are Stainless steel, 12Chromium-1Molybdenum steel and Titanium steel. These materials have a varying degree of suitability in terms of the mechanical and physical properties desired for a steam turbine blade. These were explored in order to recommend a suitable material that could be fit for the purpose of the turbine blade design. The following table indicates the properties of the materials.

Table 1: Mechanical properties of the blade materials

S/No	Material Variables	Field	Stainless Steel	Titanium Alloy	12Cr-1Mo Steel	Units
1	Density		7750	4620	7810	kg/m ³
2	Coefficient of Thermal Expansion		1.7×10^{-5}	9.4×10^{-6}	1.4×10^{-5}	C ⁻¹
3	Young's Modulus		1.93×10^{11}	9.6×10^{10}	2.06×10^{11}	Pa

S/No	Material Variables	Field	Stainless Steel	Titanium Alloy	12Cr-1Mo Steel	Units
4	Poisson's ratio		0.31	0.36	0.3	
5	Bulk Modulus		1.693×10^{11}	1.1429×10^{11}	1.7167×10^{11}	Pa
6	Shear Modulus		7.3664×10^{11}	3.5294×10^{10}	7.9231×10^{10}	Pa
7	Tensile Yield Strength		2.07×10^8	9.3×10^8	7.35×10^8	Pa
8	Compressive Yield Strength		2.07×10^8	9.3×10^8	7.35×10^8	Pa
9	Tensile Ultimate Strength		5.86×10^8	1.07×10^9	8.8×10^8	Pa
10	Isotropic Thermal Conductivity		15.1	21.9	28	$\text{W} \cdot \text{m}^{-1} \text{C}^{-1}$
11	Specific Heat		480	522		$\text{J} \cdot \text{kg}^{-1} \text{C}^{-1}$
12	Isotropic Resistivity		7.7×10^7	1.7×10^{-6}		$\Omega \cdot \text{m}$

3. Blade Static Analysis

The blade static loading analyses were carried out using the ANSYS static structural analysis system option. The effect of the steam at upstream of the last stage blade was analyzed by evaluating the various stress levels in the model. The three different blade materials were subjected to the same steam impinging conditions.

The lower part of the blade depicts the blade hub. This is very useful in the simulation study as it allows for the inclusion of the fixed support constraint. Due to the high centrifugal force on the base of the blade profile with contact at the blade hub, the mesh at this contact region is refined. This is in order to give well refined and accurate results as it is a major stress region. The image results below show the undeformed structure and the deformed blade profile after it had been subjected to the entry steam pressure of the last stage blade. Contour plots for Stainless steel, Titanium alloy and 12Cr-1Mo steel are presented in Figure 4 to Figure 15. These are plots of the Total deformation, von-Mises stress, Shear stress and the Equivalent elastic strain. A Min-Max probe was used to clearly indicate the minimum and maximum output parameter under study on the deformed blade profile. Figure 4 to Figure 6 shows the total deformation experienced by the blade materials. The result shows that Titanium alloy experienced the least deformation among the blade materials. Also, Titanium alloy had the least Von Mises stress as shown in Figure 7 to Figure 9. Stainless steel showed the best resistance to shear stress. The shear stress contours for the three materials are shown in Figure 10, Figure 11 and Figure 12. Figure 15 shows the chrome steel having the least elastic strain when compared to Figure 13 and Figure 14 for stainless steel and Titanium alloy respectively.

It was observed that the maximum von-Mises stress for the steam turbine blade analyzed with 316 Stainless steel is greater than its allowable (yield stress), which is 2.07×10^8 Pa. This is indicative of the fact that, under this operating condition, the blade will fail and, therefore, it will not be found suitable for this application, without inducing failure of the system. With the other two blades having a maximum von-Mises stress lower than their material yield stress, their suitability is then subjected to the material with the least maximum von-Mises stress according to the von-Mises stress criterion. Considering the equivalent (von-Mises) stress for the three blade materials, the contour plot for the stainless steel shows a maximum stress value of 6.2324×10^8 Pa.

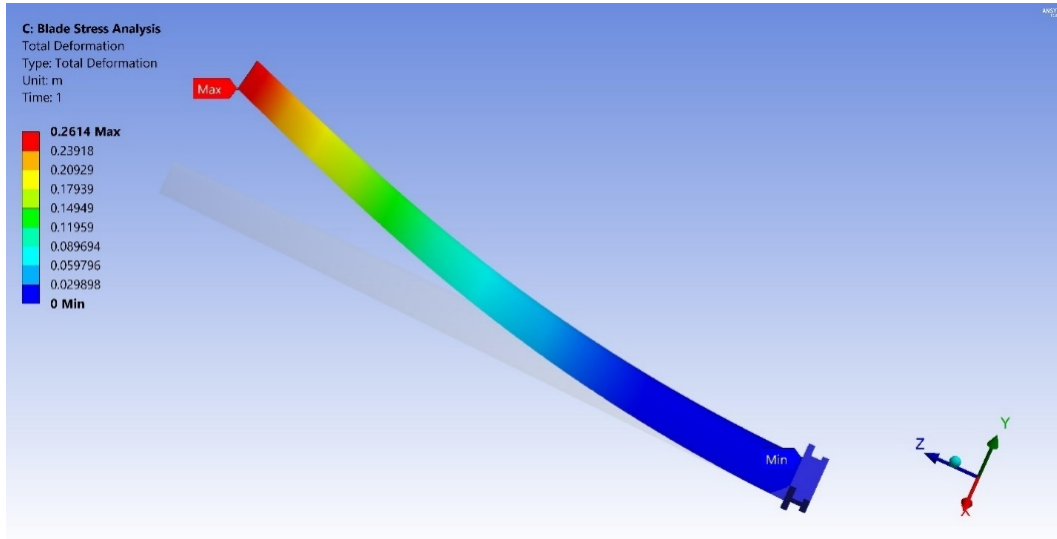


Figure 4: Total deformation contour plots for Stainless Steel

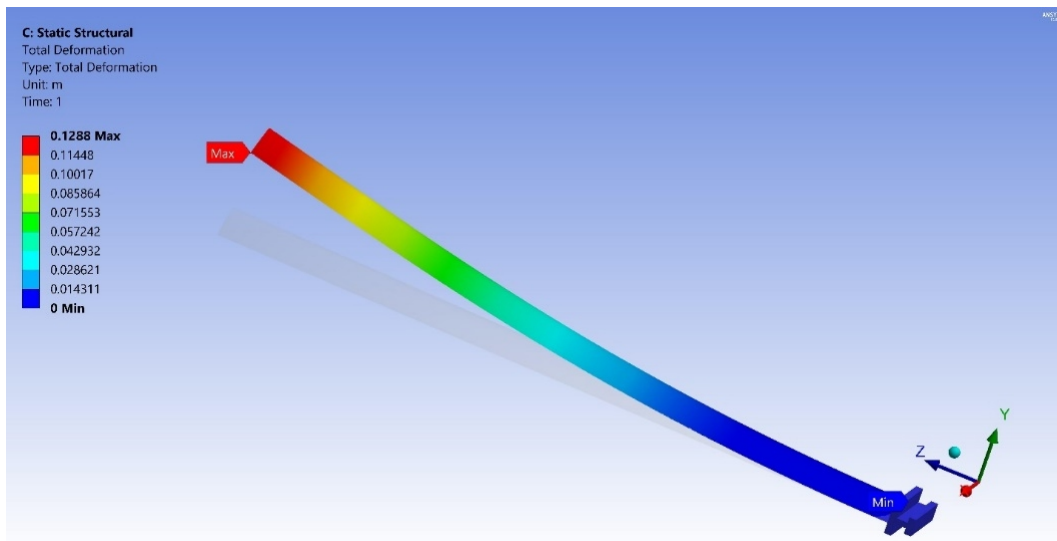


Figure 5: Total deformation contour plots for Titanium Alloy

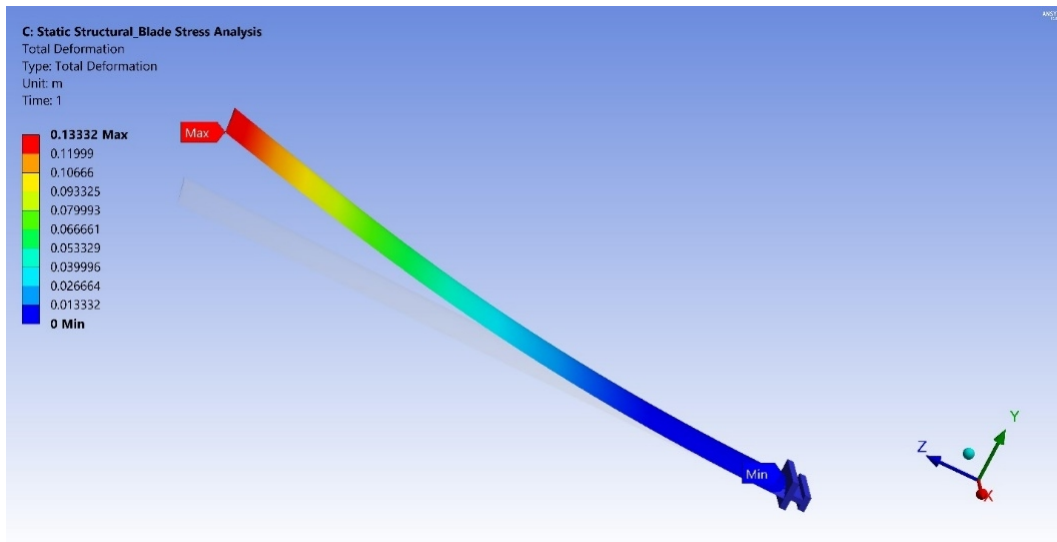


Figure 6: Total deformation contour plots for Chrome Steel

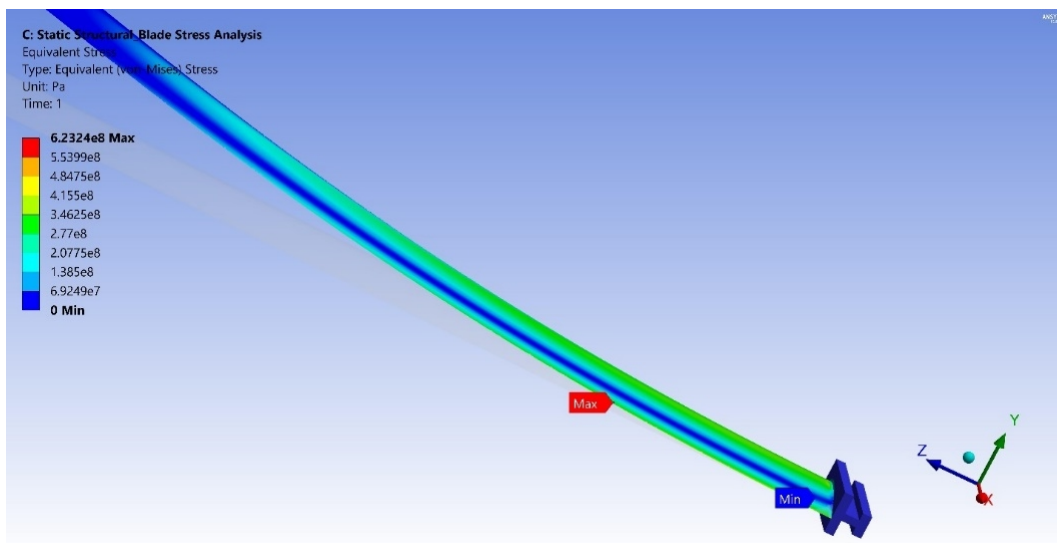


Figure 7: Von Mises stress contour plots for Stainless Steel

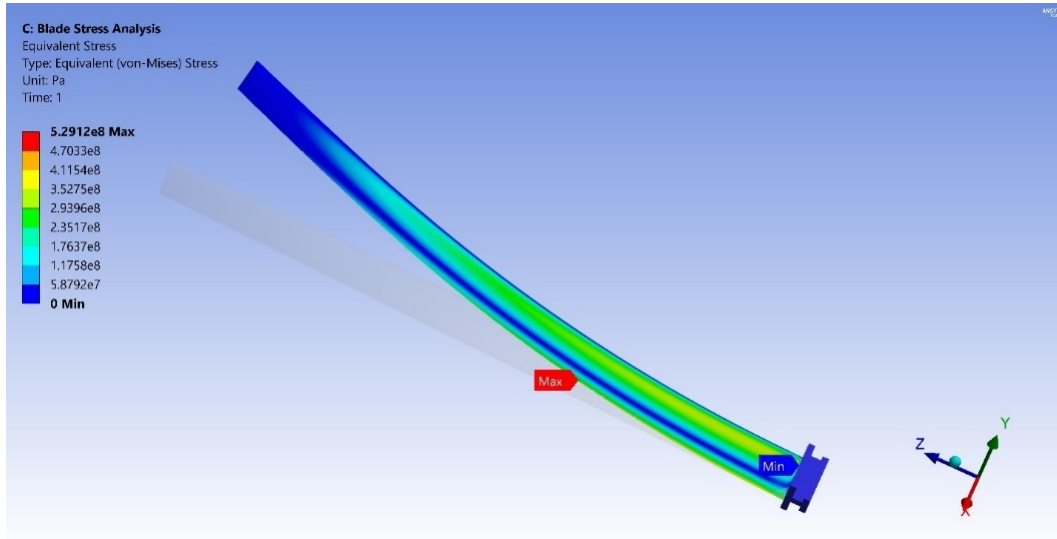


Figure 8: Von Mises stress contour plots for Titanium Alloy

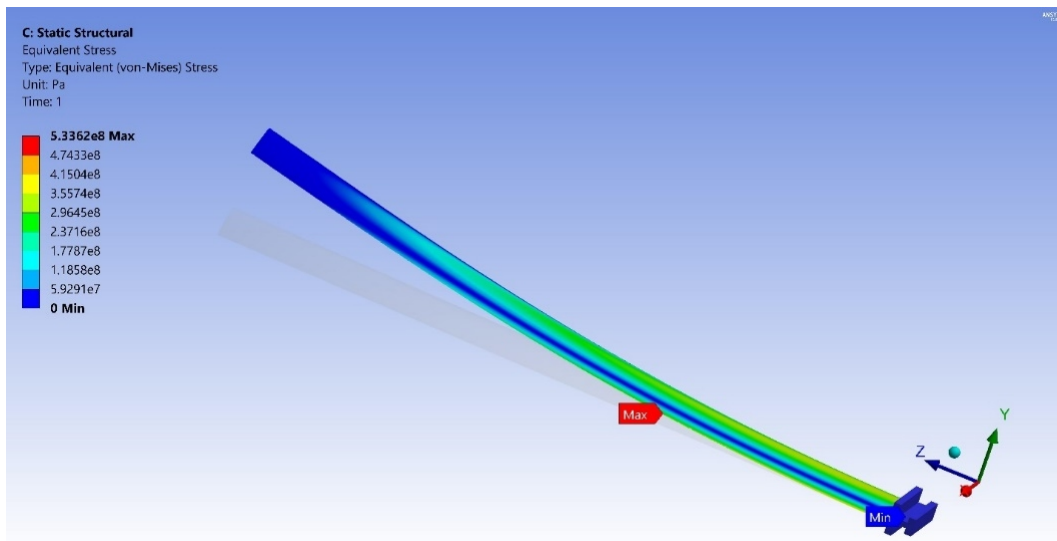


Figure 9: Von Mises stress contour plots for Chrome Steel

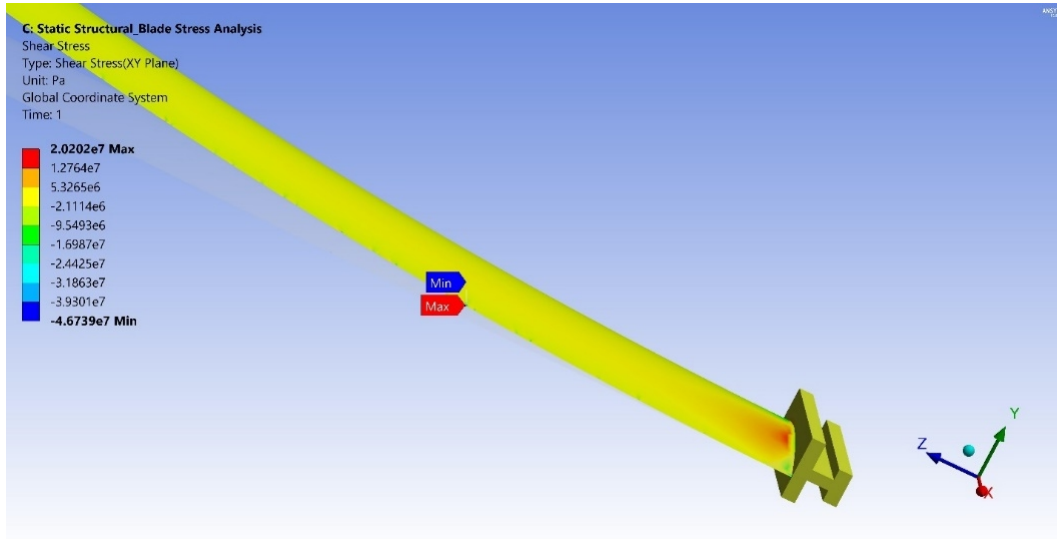


Figure 10: Shear stress contour plots for Stainless Steel

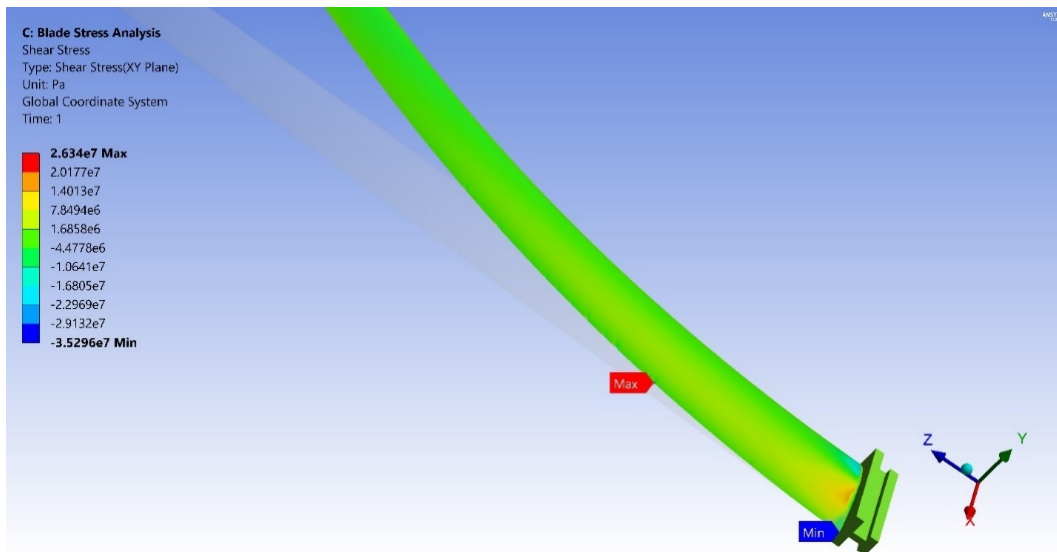


Figure 11: Shear stress contour plots for Titanium Alloy

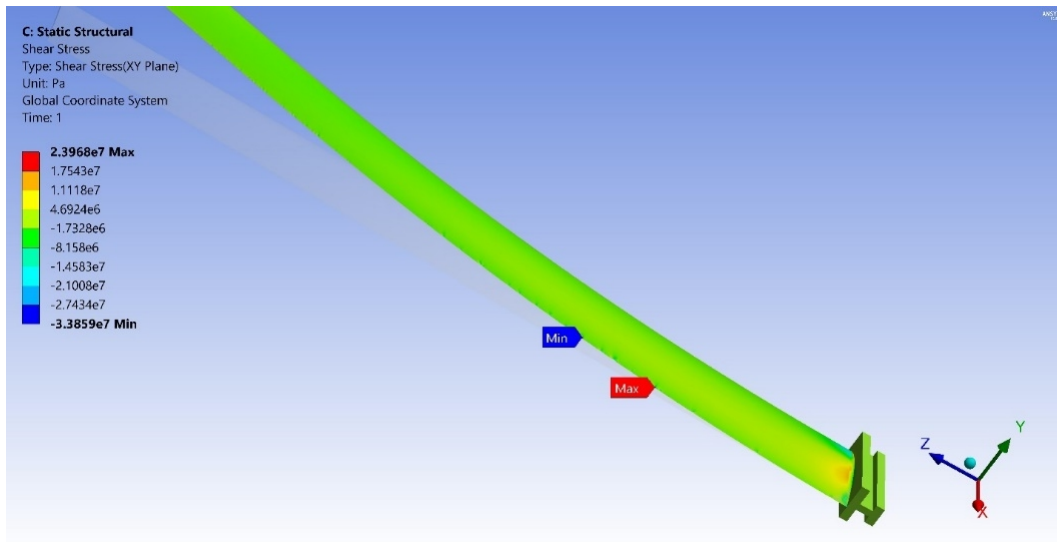


Figure 12: Shear stress contour plots for Chrome Steel

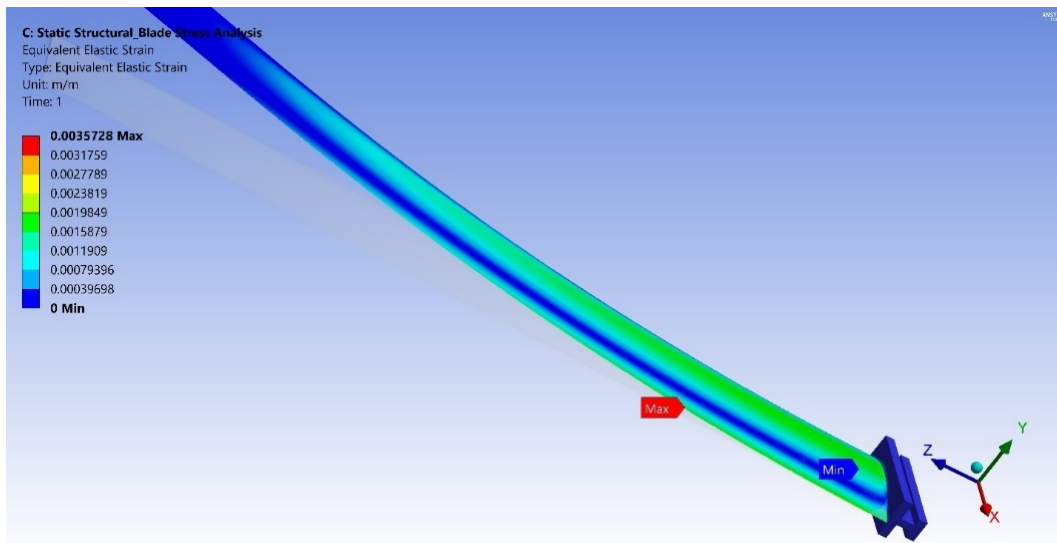


Figure 13: Equivalent elastic strain contour plots for Stainless Steel

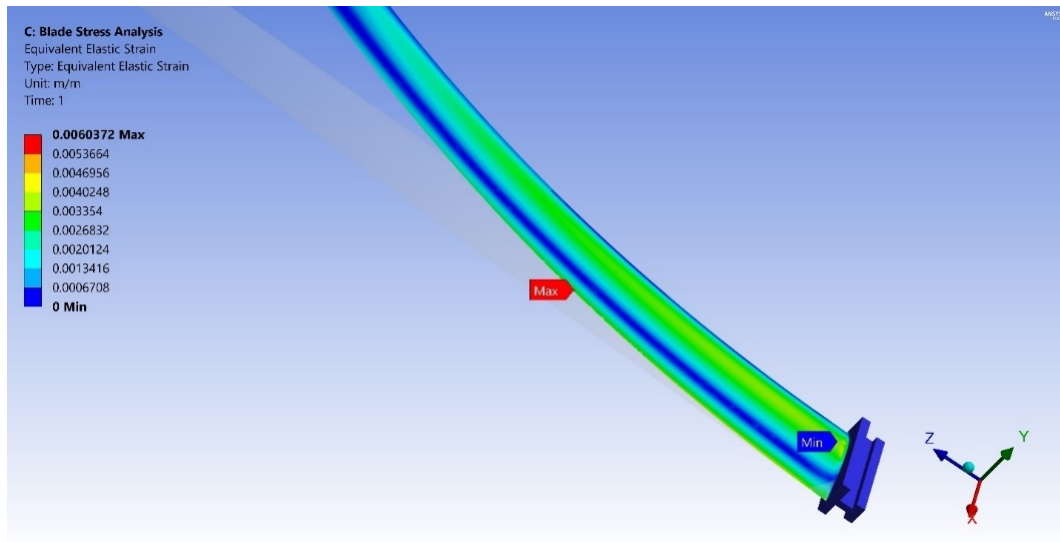


Figure 14: Equivalent elastic strain contour plots for Titanium Alloy

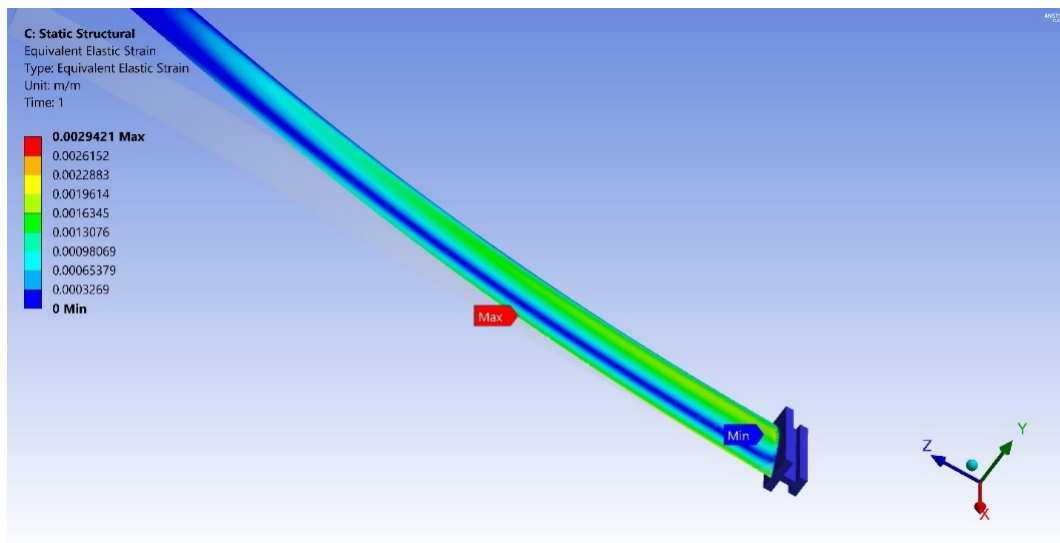


Figure 15: Equivalent elastic strain contour plots for Chrome Steel

This value is the largest compared with the other two materials in which chrome steel has a value of 5.3362×10^8 Pa and 5.2912×10^8 Pa for that of Titanium alloy. These results show that the Titanium alloy is clearly the superior material in this case as it has the least maximum von-Mises stress level. Under the supercritical thermal working conditions of the steam turbine engine, the blade with the Titanium alloy material is very much sustainable and suitable.

Considering the total deformation characteristics of the three blades, the maximum values for each material are relatively close to that of stainless steel 316, having the highest value of 0.2614 m as compared with chrome steel with deformation value of 0.1288 m and Titanium of 0.1333 m.

3.1 Response Surface

The response surface for the output variables – the equivalent shear stress and the total deformation of the Titanium alloy blade were analyzed. Titanium alloy was chosen for this analysis because it showed the best characteristics among the other materials in the previous simulation of Von mises stress, total deformation, equivalent elastic strain and shear stress. This work provides the two-dimensional response surface depictions as provided in the ANSYS response surface optimization. The optimization was done considering equivalent stress maximum (Von Mises stress) and total deformation as output variables. The total number of design points (DP) used for this study are 25 points, which are enough to capture the behaviour of the two output variables of the turbine blade in response to changes in the blade twist angle.

Table 4 shows a table for these parameters as generated by the optimal space filling (OSF) design of experiment. The negative sign in the values of the twist angles only shows the blade was twisted clockwise. The highest value of the twist in the design points is 39.5 degrees while the least twist was 11 degrees. The design point with the highest equivalent stress maximum value is at a twist angle of 11 degrees. This does not necessarily mean the twist angle at 39.5 degrees will give the least equivalent stress maximum. As can be seen in Table 4, the least equivalent stress maximum appears when the twist angle is set at 33.5 degrees with a value of 422.2 MPa. On the other hand, 11 degrees twist angle is seen to show the minimum total deformation of 0.2385 m.

Table 2: Design points generated using the Optimal Space Filling (OSF) Design of Experiments

DP	P1 - Blade Angle (degree)	Twist	P4 - Equivalent Stress Maximum (Pa)	P5 - Total Deformation Maximum (m)
1	-11		7.5580×10^8	0.2385
2	-12.5		5.6340×10^8	0.23919
3	-19		4.5777×10^8	0.24385
4	-19.5		5.2912×10^8	0.2614
5	-20.5		5.3028×10^8	0.24511
6	-21.5		5.4186×10^8	0.24595
7	-22		4.9402×10^8	0.24633
8	-22.5		5.0012×10^8	0.24678
9	-23.5		6.8217×10^8	0.24792
10	-24.5		4.9367×10^8	0.24897
11	-25.5		5.5516×10^8	0.25007
12	-26.5		4.6601×10^8	0.25114
13	-27.5		4.2628×10^8	0.25233
14	-28.2		5.3068×10^8	0.25309

DP	P1 - Blade Twist Angle (degree)	P4 - Equivalent Stress Maximum (Pa)	P5 - Total Deformation Maximum (m)
15	-29.5	4.8103×10^8	0.25489
16	-30.5	4.2997×10^8	0.25622
17	-31	5.8408×10^8	0.25694
18	-32.5	5.0600×10^8	0.25903
19	-33.5	4.2227×10^8	0.26062
20	-34.5	4.3763×10^8	0.26175
21	-35.5	7.2590×10^8	0.26299
22	-36.5	4.2922×10^8	0.26495
23	-37.5	4.3238×10^8	0.27315
24	-38	5.6721×10^8	0.26854
25	-39.5	5.4689×10^8	0.2711

Figure 16 and Figure 17 below are graphs that show the behaviour of the total deformation of the blade and the equivalent stress maximum with respect to the blade twist angle. Figure 16 clearly shows that the deformation of the blade has an inverse relationship with the blade twist angle. Figure 17 shows a rather non-uniform relationship between the equivalent stress and the blade twist angle. It is generally observed that the extreme total deformation maximum and equivalent stress maximum behaviour of the blade for range of design points considered are located at:

- (DP at 11°) → Lowest total deformation maximum value = 0.2385
- (DP at 37.5°) → Highest total deformation maximum value = 0.27315
- (DP at 33.5°) → Lowest equivalent stress maximum value = 4.2227×10^8
- (DP at 11°) → Highest equivalent stress maximum value = 7.558×10^8

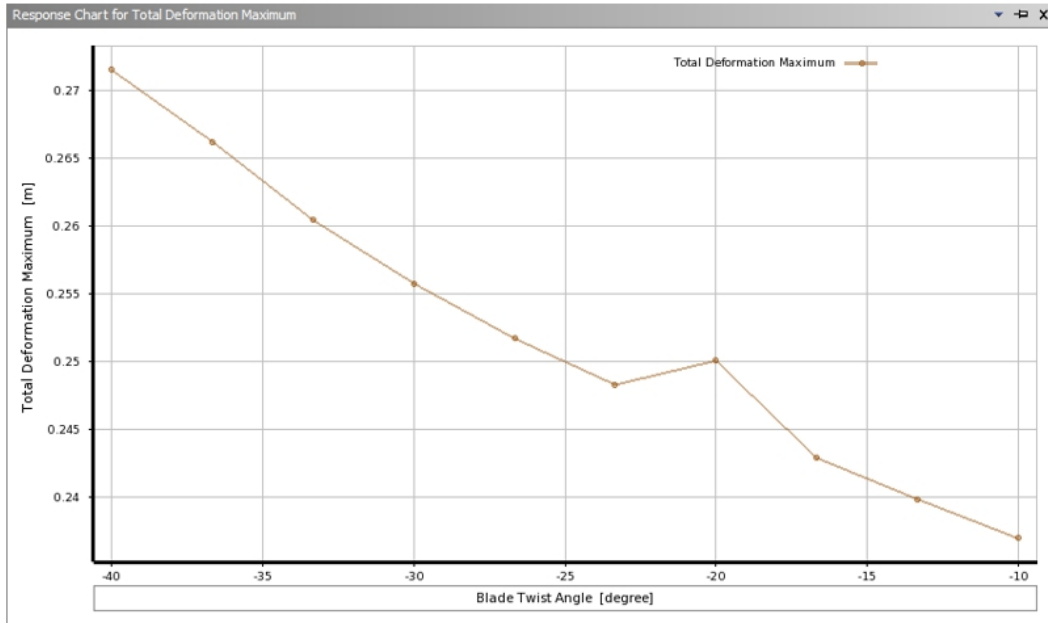


Figure 16: Response surface graph depicting the variation of the total deformation maximum with the blade twist angle

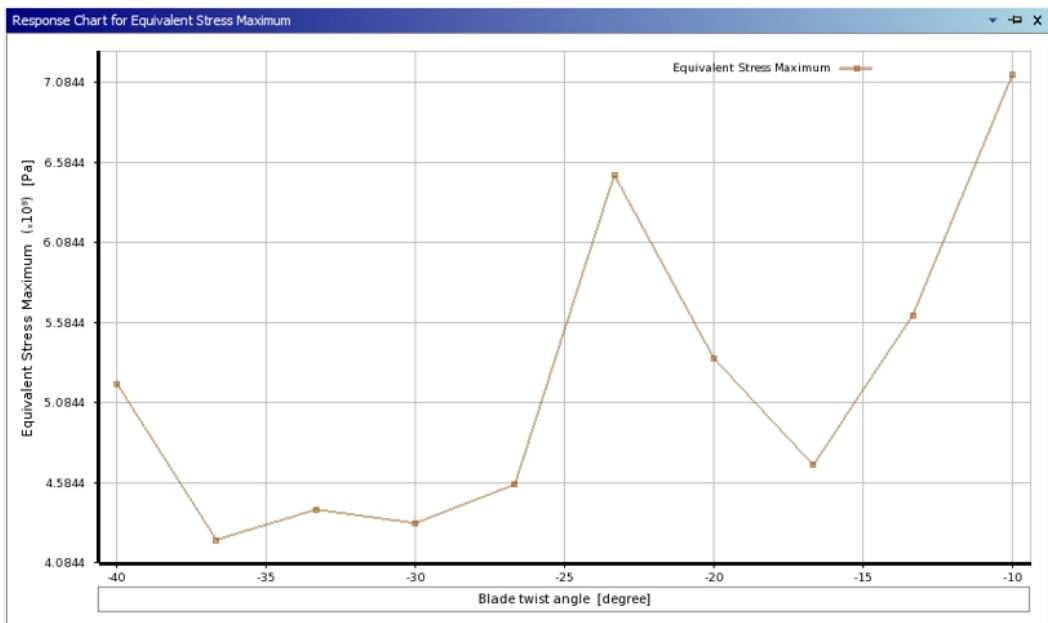


Figure 17: Response surface chart depicting the variation of the equivalent stress maximum with the blade twist angle

3.2 Optimization

The Response Surface Optimization tool (RSO) in ANSYS is based on the much-detailed operations that had already been carried out in the DoE. The RSO extracts information from the generated response surface and optimization techniques are then carried out using some in-built algorithms. Optimal results are finally approximated by the RSO. In ANSYS RSO, there are two algorithms for a multi-objective optimization, as performed in this study. They are the Screening and the Multi-Objective Genetic Algorithm (MOGA).

The Screening optimization method is based on a basic approach of sampling and sorting. It supports multiple objectives and constraints and all types of input parameters. It is used, mostly, for initial designs, which may lead to the use of other methods for more refined optimization results for accuracy purposes. It functions by generating 1000 samples and finding 3 candidates. The MOGA also supports multiple objectives and constraints and aims at finding the global optimum results. It operates by generating 100 samples initially, 100 samples per iteration and lastly, proposing 3 candidates in a maximum of 20 iterations.

The MOGA approach was used for the optimization problem because of the rigor in its approach of finding the best 3 candidates of optimization. Our aim is to find optimum design variables for the Titanium turbine blade. Thus, the objective here is to minimize the equivalent von-Mises stress maximum and also to minimize the total deformation maximum. Based on the set objectives, it can be seen that there are viable points or design parameters that can give an optimized performance of the turbine blade. Figure 18 gives 3 candidate points that illustrates the best design parameters based on the set objectives. These points are generated via ANSYS RSO by employing the MOGA scheme for optimization after 198 evaluations or iterations. According to Figure 18, it can be seen that the 3 candidate points correspond to intermediate parameter values, that is, not extreme values. Considering candidate point 1, we see that the equivalent stress increases by 2.78% as the total deformation decreases by 3.69%. The same behaviour can be observed from candidate point 2 but with a different increment and decrement rate. Even though candidate point 3 has a total deformation value of 0.25245 m, which is the highest of the 3 candidate points, a close look at the equivalent stress column suggests that it has the lowest equivalent stress maximum value.

B	C	D	E	F	G
Name	P1 - Blade twist angle (degree)	P4 - Equivalent Stress Maximum (Pa)		P5 - Total Deformation Maximum (m)	
		Parameter Value	Variation from Reference	Parameter Value	Variation from Reference
Candidate Point 1	-18.22	★★★ 4.4295E+08	2.78%	★★★ 0.24313	-3.69%
Candidate Point 2	-16.15	★★★ 4.8958E+08	13.60%	★★★ 0.24242	-3.97%
Candidate Point 3	-27.25	★★★ 4.3098E+08	0.00%	— 0.25245	0.00%

Figure 18: The 3 candidate points proposed by ANSYS RSO with minimization of the two output variables

For the application of these candidate points in the manufacture of turbine blade, it is important to examine the effect of the maximum equivalent stress and the total deformation maximum on the overall design and efficiency of the turbine. The yield stress of Titanium alloy as seen in Table 1 is 930 MPa. The maximum equivalent stress from the three candidate points blade twist angles are roughly about 50% lesser than the yield stress. This implies that fracture cannot take place using any of these twist angles for this application. The maximum total deformation, however, has a direct impact in the design and efficiency of the turbine. The deformation will give rise to energy loss as some of the steam will flow away from the blade.

Also, when elongation is experienced as a result of the deformation, it affects the design of the casing of the turbine. This makes the maximum total deformation the most important criterion for selecting the best twist angle of the blade.

4. Conclusion

This paper has sought to achieve an optimized twist angle for the turbine blade of the last stage low pressure steam turbine using ANSYS CFD simulation software. The main aim is to improve the efficiency of existing steam turbines. This is to be achieved by modelling an existing steam turbine blade, evaluating its influence and proposing alternative materials and twist angles.

Static analysis of the blade was carried out using the 3D model. Three different materials (Titanium alloy, stainless steel and Chromium 12) were studied. The mechanical properties of the chosen blade materials were compared. The stresses experienced by these materials were examined. The mechanical properties examined include the Von Mises stress, total deformation, shear stress, equivalent elastic strain. From the simulation it is believed that Titanium alloy shows the best mechanical properties in terms of resistance to the stresses experienced by the blade during operation.

Since Titanium alloy showed the best properties, it was used to simulate different twist angle for the blade. 25 DPs were chosen, and an optimization simulation was carried out using MOGA. The result shows three candidate points representing the best twist angles and their values. The result also gave the corresponding equivalent stress maximum (Von Mises stress) and the maximum total deformation at the candidate points. Candidate point two with a twist angle of 16.15 degrees is seen to have the best minimization values for the two output variables.

Acknowledgements

Parts of the research for this paper were undertaken while the corresponding author was employed as a Project engineer at Nestle Nigeria, Plc. The author thanks Nestle for its support in undertaking this research work. The authors also wish to acknowledge the support offered by Egbin thermal power station in the actualization of this research work for publication.

References

- [1] Singh, M. P., and Lucas, G. M. (2011). *Blade Design and Analysis for Steam Turbines*. The McGraw-Hill Companies, New York.
- [2] Fadla, M., Steinb, P., and Hea, L. (2017). Full conjugate heat transfer modelling for steam turbines in transient operations. *International Journal of Thermal Sciences*, 124, 240-250.
- [3] Bloch, H. P., and Singh, M. P. (2009). *Steam Turbines; Design, Applications, and Rerating*. The McGraw-Hill Companies, New York.

- [4] Naumann, H. G., (1982). Steam turbine blade design options: how to specify or upgrade. In Proceedings of the 11th Turbomachinery Symposium. Texas A&M University. Turbomachinery Laboratories.
- [5] Chaplin, R. A. (2011). Steam Turbine Impulse and Reaction Blading. Thermal Power Plants, 3, 57-87.
- [6] Saito, E. I. J. I., Matsuno, N. A. R. I. Y. U. K. I., Tanaka, K. E. I. Z. O., Nishimoto, S. H. I. N., Yamamoto, R. Y. U. I. C. H. I. and Imano, S. H. I. N. Y. A., 2015. Latest technologies and future prospects for a new steam turbine. Mitsubishi Heavy Industries Technical Review, 52(2), 39-46.
- [7] Nagaraju, G., Mamilla, V. R., Mallikarjun, M. V. (2013). Design optimization and static and thermal analysis of gas turbine blade. International Journal of Engineering, Business and Enterprise Applications, 5(1), 53-57.
- [8] Senoo, S., Ono, H., Shibata, T., Nakano, S., Yamashita, Y., Asai, K., Sakakibara, K., Yoda, H. and Kudo, T., 2014. Development of titanium 3600rpm-50inch and 3000rpm 60inch last stage blades for steam turbines. International Journal of Gas Turbine, Propulsion and Power Systems, 6(2), 9-16.
- [9] Anderson-Cook, C. M., Montgomery, D. C., Meyers, R. H. (2016). Response Surface Methodology: Process and Product Optimization using Designed Experiment, 4th Edition. John Wiley & Sons, Hoboken, New Jersey.
- [10] Venter, G., Haftka, R. and Starnes, Jr, J., (1996). Construction of response surfaces for design optimization applications. In 6th Symposium on Multidisciplinary Analysis and Optimization, American Institute of Aeronautics and Astronautics Inc., Paper 96-4040, 548-564.